JPET Fast Forward. Published on June 24, 2019 as DOI: 10.1124/jpet.119.258053
This article has not been copyedited and formatted. The final version may differ from this version.

TITLE PAGE

Implication of K_v7 channels in the spinal antinociceptive actions of celecoxib[1].

Jorge Vicente-Baz, BS, Jose A. Lopez-Garcia, PhD, Ivan Rivera-Arconada, PhD

Department of Systems Biology (Physiology), Universidad de Alcala, Alcala de Henares, Madrid, Spain.

Affiliation: JVB; JALG and IRA: Department of Systems Biology (Physiology), Universidad de Alcala, Alcala de Henares, Madrid, Spain.

JPET Fast Forward. Published on June 24, 2019 as DOI: 10.1124/jpet.119.258053
This article has not been copyedited and formatted. The final version may differ from this version.

RUNNING TITLE PAGE

Running Title: Spinal effects of celecoxib mediated by K_V7 channels

Corresponding author:

Ivan Rivera Arconada

Dpt. Biología de Sistemas (Área Fisiología)

Edificio de Medicina, Campus Universitario

Carretera N-2 Km 33.600

Universidad de Alcalá

Alcalá de Henares

28805 Madrid, Spain

Telephone + 34 91 885 5106

Fax +34 918854807

E-mail: ivan.rivera@uah.es

Number of text pages: 31

Number of tables: 0

Number of figures: 6

Number of references: 47

Number of words in Abstract: 237

Number of words in Introduction: 411

Number of words in Discussion: 1228

Nonstandard abbreviations: aCSF, artificial cerebrospinal fluid; COX, cyclooxygenase; DMC, 2,5-dimethyl-celecoxib; DMSO, dimethyl sulfoxide; MEA, multielectrode array; MSR, monosynaptic reflex; NSAID, non-steroidal anti-inflammatory drug;

Recommended section: Neuropharmacology

JPET Fast Forward. Published on June 24, 2019 as DOI: 10.1124/jpet.119.258053
This article has not been copyedited and formatted. The final version may differ from this version.

Abstract

Celecoxib is an NSAID commonly used to treat pain conditions in humans. In addition to its blocking activity on COXs enzymes, several other targets could contribute to its analgesic activity. Here we explore the spinal antinociceptive actions of celecoxib and the potential implication of K_v7 channels in mediating its effects. Spinal cord *in vitro* preparations from hind paw-inflamed animals were used to assess the segmental sensory-motor and the early sensory processing of nociceptive information. Electrophysiological recordings of ventral roots and dorsal horn neurones were obtained and the effects of celecoxib and K_v7 modulators on responses to repetitive dorsal root stimulation at C-fibre intensity were assessed. Celecoxib applied at clinically relevant concentrations produced depressant effects on responses to dorsal root stimulation recorded from both ventral roots and individual dorsal horn neurones, in contrast the non-nociceptive monosynaptic reflex was unaffected. The NSAID indomethacin was devoid of effect on spinal reflexes, but further co-application of celecoxib still produced depressant effects. The depressant actions of celecoxib were abolished after K_v7 channel blockade and mimicked by its structural analogue dimethyl-celecoxib that lacks COX blocking activity. The present results identify K_v7 channels as novel central targets for celecoxib that may be relevant to its analgesic effect. This finding contributes to better understand the pharmacology of celecoxib, and reinforces both the role of K_v7 channels in modulating the excitability of central pain pathways and its validity as target for the design of analgesics.

Introduction

Celecoxib is a non-steroidal anti-inflammatory drug (NSAID) with selective activity on cyclooxygenase 2 (COX-2) isozymes, that is indicated for the treatment of rheumatoid arthritis and osteoarthritis in humans (Clemett and Goa, 2000). Celecoxib applied systemically is effective in reducing nociceptive behaviours in various animal models of pain, including the formalin test and the carrageenan model of paw-inflammation (Inoue et al., 2009; Penning et al., 1997; Smith et al., 1998; Sun et al., 2013; Zhang et al., 1997). In addition, the application of celecoxib and other NSAIDs by intrathecal route also produce antinociceptive effects in the same models (Dirig et al., 1998; Lee and Seo, 2008; Malmberg and Yaksh, 1992; Nishiyama, 2006). These reports suggest that, in addition to peripheral actions, the spinal cord may be a relevant site for NSAIDs-induced analgesia. Further to its COX blocking actions, celecoxib has been reported to interact with opioid and cannabinoid systems as well as a variety of ionic channels (Brueggemann et al., 2009; Du et al., 2011; Frolov and Singh, 2014; Park et al., 2007; Rezende et al., 2012).

Of special interest for nociceptive processing, celecoxib affects the activity of voltage dependent potassium channels of the K_V7 family (Du et al., 2011). These channels are expressed in peripheral and central elements of the nociceptive system (Rivera-Arconada et al., 2009) and their modulation alters the excitability of primary afferents and spinal neurones due to its fundamental role regulating membrane resting potential and repetitive firing (Jentsch, 2000; Passmore et al., 2003; Rivera-Arconada and Lopez-Garcia, 2005). The K_V7 channel opener retigabine applied systemically shows analgesic-like effects on animal models of inflammatory, visceral, neuropathic and cancer pain

(Blackburn-Munro and Jensen, 2003; Hirano et al., 2007; Passmore et al., 2003; Zheng et al., 2013). Application of celecoxib to dorsal root ganglion neurones *in vitro* produces an enhancement of K_v7-mediated currents, an effect that may be relevant to its analgesic actions (Mi et al., 2013).

Here we explore the potential contribution of K_v7 channels expressed in spinal neurones to the analgesic effects of celecoxib. To this end, we used electrophysiological recordings of spinal reflexes and dorsal horn neurones in an *in vitro* preparation of the mouse spinal cord obtained after the induction of inflammation. The effect of celecoxib on spinal function was assessed and the contribution of K_v7 channels was tested using a variety of pharmacological tools. Our results are in agreement with the hypothesis that modulation of K_v7 channels is relevant to the spinal antinociceptive actions of celecoxib.

Methods

All experimental protocols were performed following European Union and Spanish Government regulations for animal handling, were approved by the local Ethics Committee and the Govern of the Community of Madrid (Ref. PROEX 018/16) and comply with the ARRIVE guidelines. Experiments were performed on 6 to 11-day-old CD1 mice of either sex weighing between 4 and 9.7 g. Animals were breed in-house, kept together with their mothers and maintained under a light-dark cycle of 12 h:12 h with 55 ± 15% humidity. The number of animals used was kept to the minimum that allowed a clear interpretation of main results. All efforts were made to minimize animal suffering.

Induction of peripheral inflammation and behavioural testing

Peripheral inflammation was induced by intraplantar injection of carrageenan (3% in saline; 30 µl) in both hind paws. This procedure ensured maximum inflammation and allowed to use either side of the cord in electrophysiological experiments. Paw diameters and mechanical withdrawal thresholds were measured before and 20h after carrageenan injection. Withdrawal threshold was defined as the minimum mechanical force applied with von Frey filaments (from 0.008 to 2 g) that elicited a withdrawal response in at least 3 out of 5 trials. For statistical analysis, threshold and paw diameter of the hind paw ipsilateral to the hemi cord used for electrophysiological recordings were considered.

In vitro spinal cord preparations and dorsal root stimulation

Mice were anaesthetised with urethane (2 mg kg^{-1}, i.p.) and their spinal cords extracted after a dorsal laminectomy following a procedure described in full elsewhere (Lopez-Garcia and Laird, 1998). The whole cord was used for recording spinal reflexes. The spinal cord was hemisected to make multielectrode recordings from deep dorsal horn neurones. To record neurones located in superficial laminae, the lumbar enlargement of the whole spinal cord was sliced in a vibratome to obtain a single slice of ≈400 µm containing the dorsal part of the cord (laminae from I to V) together with the attached dorsal roots. In the recoding chamber the cord was pinned down to the Sylgard base of a recording chamber with the medial or sectioned side upward to facilitate electrode penetration. Cords were continuously superfused (4-6 mL min^{-1}) with oxygenated (95% O_2; 5% CO_2) artificial cerebrospinal fluid (aCSF) at room temperature (22 ± 1ºC). The composition of the aCSF was (in mM): NaCl (127), KCl (1.9), KH_2PO_4 (1.5), $MgSO_4$ (1.3), $CaCl_2$ (2), $NaHCO_3$ (22), glucose (10); pH 7.4.

Electrical stimuli were applied to the L4 dorsal root via thigh fitting glass suction electrodes. Electrical stimulation consisted of a train of 15 consecutive C-fibre intensity stimuli (200 µA, 200 µs) applied at 1 Hz to produce wind-up responses. Trains of stimuli were applied at 30 min intervals.

Ventral root reflex recordings

The L4 ventral root was placed in a tight-fitting glass suction electrode. Signals were obtained using a Multiclamp 7A amplifier (Molecular Devices, California, USA), sampled at 6 kHz and stored for analysis using Spike 2 software (CED,

Cambridge, UK). Depolarisation of motoneuronal populations was recorded in DC channel. Repetitive dorsal root stimulation at C-fibre intensity produced a cumulative depolarisation. For each of the 15 stimuli, amplitude from baseline was measured at the end of the response. Integrated area under the curve during the 24 s following the first stimulus artefact was measured to quantify the cumulative depolarisation. Electrical stimuli elicited a monosynaptic reflex (MSR) at 5-10 ms from stimulus artefact. The MSR was quantified as amplitude from baseline using the first stimulus of the train.

Digital band-pass filtering of the original DC signal between 200 and 1200 kHz allowed to generate an AC channel collecting fast spike-like events produced by the firing of action potentials in motor neurones (Rivera-Arconada et al., 2016). Events crossing an amplitude threshold were counted in a time window between 100 and 950 ms from stimulus artefact and summated to obtain total spike counts to each train of stimuli. Stable baseline responses were usually obtained after 2-4 repetitions.

Multielectrode recordings from dorsal horn neurones and estimation of recording sites.

Multielectrode arrays (MEAs; A4×4 3 mm-50/100-125-177-A16 or Buzsaki32; Neuronexus Technologies, USA) had 4 shanks with 4-8 iridium recording sites separated by 30–100 µm. MEA tips were placed under visual guidance and introduced using a remote-controlled micromanipulator. For recordings of deep dorsal horn neurones, extracellular signals were preamplified ×10 (MPA81, Multichannel Systems, Germany) and further amplified x500 with an 8-channel amplifier (Cyberamp, Molecular Devices, California, USA; (Roza et al., 2016). In

recordings from superficial dorsal horn neurones, the electrode was connected to a RHS2000 32-channel headstage containing two RHS2116 amplifier chips (Intan Technologies, USA; (Lucas-Romero et al., 2018). The signals were, band-pass filtered between 200-300 Hz and 3 kHz, digitized at 20 kHz (1401 Plus, CED, UK), and stored for analysis.

Spike sorting was performed offline based on spike shape parameters using Spike 2. Only data obtained from unequivocally classified units was considered as single unit activity. One to five neurones were isolated from each experiment. Action potentials elicited by dorsal root stimulation were counted excluding the 50 ms following stimulus artefact. Drugs were applied only if responses to repetitive stimuli were stable during 2 or 3 stimulation cycles. Responses of dorsal horn neurones recorded with MEAs were reproducible during long lasting (1.5 h) applications of the solvent DMSO (12 neurones from 3 different preparations).

To estimate the position of the deep dorsal horn neurones recorded, the electrode position inside the cord was estimated by DiI labelling (Sigma-Aldrich, Madrid, Spain). At the end of a successful track, a microelectrode with identical characteristics stained with DiI was placed in the micromanipulator and lowered to the recording position. This electrode substitution was performed to avoid unnecessary exposition of neurones to DiI and to prevent damage to the recording electrode. Then, the spinal cord was fixed by immersion in 4% paraformaldehyde, embedded in gelatine and sectioned in a cryostat at 100 µm. DiI fluorescence was visualized directly onto sectioned tissue and the depth and trajectory of the electrode were recovered (Roza et al., 2016). In recordings from superficial dorsal horn neurones, the distance of the electrode tip to the

dorsal border of the spinal cord was measured with the micromanipulator. After the recording session, the slice was fixed in 4% paraformaldehyde, embedded in gelatine and sectioned in a cryostat at 30 µm. Then sections were stained with toluidine 0.1% and dehydrated to obtain an estimation of the laminae contained in the slice.

Drugs and chemicals

Carrageenan lambda, celecoxib, XE-991, indomethacin, 2,5-dimethyl-celecoxib (DMC) and the components for the aCSF were purchased from Sigma-Aldrich (Madrid, Spain). Linopirdine was acquired from Tocris Bioscience (Bristol, UK). The aCSF was freshly prepared for each experiment. The compounds were prepared in DMSO as concentrated stock solutions (10-20 mM) and stored at -20 ºC. All compounds were diluted down to the final concentration in aCSF just prior to use and superfused to the entire preparation for at least 25 min periods to ensure a complete tissue equilibration.

To study the effect of the compounds, each preparation received applications of only one of the compounds at a maximum of three increasing concentrations. In experiments designed to assess the implication of COX enzymes, 10 µM indomethacin was applied during 60 min and then 10 µM celecoxib was added to the perfusion medium. In other series of experiments, the K_v7 channel blockers XE-991 or linopirdine were superfused for 60-90 minutes before the application of celecoxib or DMC.

Statistical analysis

Statistical analysis was performed with GraphPad Prism (GraphPad Software, California, USA). All data are presented as mean ± SEM unless otherwise

stated. Analysis of data from behavioural assays were made using Wilcoxon matched pairs test. The effects of celecoxib on spinal reflexes were first compared to control experiments with DMSO applications using the same three concentrations schedule, to avoid a misinterpretation of drug actions due to the long lasting protocol employed. These comparisons were done using a Two-Way ANOVA test with data normalized to pre-drug (or pre-solvent) values. Concentration dependent effects of the drugs from pre-drug values were analysed in raw data using Bonferroni *post-hoc* test after repeated measures One-Way ANOVA. For electrophysiological studies with a single concentration of drug comparisons to pre-drug values were performed using paired *t*-test analysis.

Results

Celecoxib actions on spinal reflexes recorded from paw inflamed mice

Intraplantar injections of carrageenan induced an inflammatory process in mice pups characterised by paw swelling and allodynia. Twenty hours after carrageenan injection, paw diameter increased from 2.18 ± 0.02 mm to 2.68 ± 0.06 mm ($p < 0.001$; Wilcoxon test, $n = 58$) and mechanical withdrawal thresholds assayed with von Frey filaments were reduced from a median force of 1 g to 0.04 g ($p < 0.001$; Wilcoxon test, $n = 58$).

After spinal cord extraction, spinal reflexes elicited by dorsal root stimulation were recorded from the ventral root. Repetitive dorsal root stimulation at C-fibre intensity induced a progressive potentiation of the responses recorded from the ventral root that manifested as a cumulative depolarisation associated to spike wind-up (fig 1A). Integrated area of cumulative depolarisation and spike wind-up were analysed to assess drug effects on nociceptive transmission. The effects of celecoxib at three different concentrations (1, 3 and 10 µM; $n = 10$) were compared to those of the solvent DMSO applied with the same protocol in a separate series of experiments ($n = 5$). A two way analysis of variance detected significant depressions produced by celecoxib on the cumulative depolarisation ($F(1,13) = 13.34$; $p = 0.003$) and the associated spike wind-up ($F(1,13) = 8.53$; $p = 0.012$). The effects of celecoxib were concentration-dependent and, compared to pre-drug values, effects on both cumulative depolarisation and spike wind-up were statistically significant at concentrations ≥ 3 µM (fig 1C-E).

Dorsal root stimulation caused, in addition, the activation of thick myelinated fibres of muscle origin producing a monosynaptic reflex (MSR) recorded from

the ventral root as a short latency peak (fig 1B). Celecoxib did not have significant effects on the MSR ($F(1,10) = 0.86$, $p = 0.38$).

To evaluate the contribution of COX block on celecoxib's actions, we used the irreversible COX blocker indomethacin (Rome and Lands, 1975). To this end, indomethacin was applied at 10 µM during 1 hour and then 10 µM celecoxib was co-applied during 30 minutes. Indomethacin alone showed no significant effects in cumulative depolarisation or spike wind-up (fig 2A-B). However, further application of celecoxib produced a significant depression of both parameters compared to values obtained under indomethacin (fig 2A-B).

Implication of K_v7 channels in the actions of celecoxib on spinal reflexes

The previous results suggest that depressant effects of celecoxib on spinal nociceptive reflexes are mediated by a COX-independent mechanism. To test the possible contribution of K_v7 channels, we studied the effect of K_v7 channel blockade on the depressant action of celecoxib. Superfusion of the K_v7 channel blocker XE-991 at 10 µM on its own produced a strong increase in spike wind-up, but not on the underlying cumulative depolarisation (n = 7; fig 3A-B). The depressant effects of celecoxib were fully abolished after K_v7 blockade with XE-991 (fig 3A-B). Similar results were obtained using linopirdine, another blocker of K_v7 channels (n = 4; fig 3C).

To further confirm the implication of K_v7 channels on celecoxib effects, we superfused the cord with DMC, an analogue of celecoxib devoid of activity on COX enzymes. DMC applied at 10 µM strongly depressed nociceptive transmission (n = 5, fig 4A-B). As observed with celecoxib, previous block of K_v7 channels prevented all depressant actions of DMC (n = 3, fig 4C).

Effects of celecoxib on the responses of dorsal horn neurones

A first series of experiments was conducted to address the potential effects of celecoxib on the spinal sensory neurones that contribute to the initial steps of sensorimotor processing. Extracellular recordings with MEAs were obtained from deep dorsal horn neurones using a hemisected spinal cord preparation that allowed to gain access directly to the gray matter. Twenty-four neurones were successfully isolated from 18 hemisected cords. Recording sites recovered after DiI labelling and histological processing showed that electrode tracks were located in lamina IV to VI, between 223 µm and 436 µm from the medial side (fig 5A).

Celecoxib was applied at 3 and 10 µM to 13 neurones. Repetitive dorsal root stimulation elicited wind-up responses in 3 neurones, whereas another 8 neurones were able to maintain spike firing during the train of stimuli and the remaining 2 neurones showed a spike wind-down. In 9 of them, action potential firing in response to C-fibre stimulation was depressed by ≥ 20% (fig 5B and D). Pooling together data from all neurones we obtained statistically significant differences at both concentrations. The four neurones insensitive to celecoxib showed a pattern of maintained firing in response to repetitive dorsal root stimulation.

Occlusion experiments with XE-991 were performed to explore the involvement of K_V7 channels in the effects of celecoxib. Responses to repetitive stimulation in pre-drug conditions for the five neurones tested included wind-up responses (2), neurones maintaining spike firing (2) and one neurone showing spike wind-down. A 60 min application of XE-991 at 10 µM produced a mild but significant change in neuronal responses to repetitive stimuli (n = 5). Following the

superfusion of XE-991, applications of celecoxib at 3 and 10 µM were completely devoid of effects in the 5 neurones tested (fig 5C and E).

In an additional set of experiments, we wanted to explore the effects of celecoxib on neurones more specifically related to nociceptive processing. Using a slice containing the laminae from I to V of the dorsal horn, we obtained MEAs recordings of the activity of superficial dorsal horn neurones in response to repetitive dorsal root stimulation at C-fibre intensity. Twenty-one superficial dorsal horn neurones were isolated from 8 spinal cord slices. Electrode tips were situated at 20-60 µm from the dorsal border of the spinal cord, allowing all the sensors to be located within laminae I-III (see fig 6A).

Celecoxib applied at 10 µM depressed the responses to dorsal root stimulation in 10 out of 12 neurones tested (fig 6B and D). Neurones inhibited by celecoxib showed wind-up (2), wind-down (3) or maintained (5) responses to repetitive stimulation. Two more neurones insensitive to celecoxib had wind-up responses.

Occlusion experiments with XE-991 were made in 9 additional neurones showing wind-up (5), wind-down (2) or maintained firing (2). XE-991, applied at 10 µM during 60 min, produced slightly increased responses in 7 neurones, but this trend did not reach statistical significance. The posterior co-application of 10 µM celecoxib was devoid of effects in the 9 neurones tested (fig 6C and E).

Discussion

Applications of celecoxib to the *in vitro* mouse spinal cord produced a concentration-dependent depression of nociceptive reflexes, manifested as a reduction of action potential wind-up and the underlying cumulative depolarisation, a model widely used to study nociceptive processing in the spinal cord (Herrero et al., 2000). On the other hand, the monosynaptic reflex, a purely non-nociceptive response, was unaffected by celecoxib. This profile of action on spinal reflexes is very similar to that of other analgesics including morphine (Mazo et al., 2015). In addition, celecoxib reduced the firing of dorsal horn neurones in response to C-fibre stimulation, indicating a specific action of the compound on sensory neurones. These results are in line with previous reports showing that celecoxib applied by intrathecal route reduces nociceptive behaviours evoked by formalin injection in the hind paws (Lee and Seo, 2008; Nishiyama, 2006).

The present results show significant depressant effects of celecoxib at concentrations ≥ 3 μM. These are in range with plasmatic levels of celecoxib achieved in humans after treatment (100-400 mg, 1-4 μM (Davies et al., 2000)) which suggest that spinal actions of celecoxib may be relevant to its analgesic effects under clinical conditions. In this work, carrageenan inflamed mice were used in an attempt to maximize COX activity. Both COX isozymes are constitutively present in the spinal cord and their expression appears to upregulate under neuropathic and inflammatory processes (Hay and de Belleroche, 1997; Zhu and Eisenach, 2003). However, some reports suggest that spinal COX activity is not relevant to acute pain transmission nor to the maintenance of hyperalgesia in inflammatory models (Dirig et al., 1998; Vardeh et al., 2009; Yamamoto and Nozaki-Taguchi, 1996). This view is reinforced by

the lack of effect of indomethacin on spinal reflexes and the large, likely unspecific concentrations, of other NSAIDs required to cause depression (Lizarraga et al., 2006; Lopez-Garcia and Laird, 1998).

Our carrageenan inflamed mice showed signs of oedema and allodynia. Previous reports using this *in vitro* model have shown larger spinal reflexes in treated rats than in controls (Hedo et al., 1999). In our hands, the application of indomethacin at 10 µM, a concentration above its therapeutic range and IC_{50} values for COX inhibition (Kalgutkar et al., 2000; Kurumbail et al., 1996; Lucas, 2016), was devoid of effect on spinal reflexes, whereas subsequent co-application of celecoxib produced clear depressant actions. These observations suggest a minor role for COX blockade in the actions of celecoxib on spinal transmission and a likely contribution of other unspecific targets for this compound.

Celecoxib applied at concentrations similar to those used in the present experiments has been shown to exert direct actions on heterologous expressed K_v7 channels and on native M-currents expressed in dorsal root ganglia neurones (Brueggemann et al., 2009; Du et al., 2011; Mi et al., 2013). A recent report has shown that K_v7 subunits 2, 3 and 5 are present in the spinal cord, and are expressed in both inhibitory and excitatory dorsal horn neurones (Häring et al., 2018). Interestingly, the authors found that the $K_v7.5$ subunit is expressed in two populations of glutamatergic neurones (glut 11 and 12) that became activated by noxious thermal stimulation. In this line, other work employing a similar approach (Sathyamurthy et al., 2018) also reported the expression of $K_v7.5$ subunits in a population of excitatory neurones (DE-7) that express Fos gene after formalin application.

Celecoxib can interact with several homo- and heteromeric conformations of K_v7 channels showing EC_{50} values between 2 and 5 μM. Celecoxib shifts the activation curve of K_v7-mediated currents to the left and produces an approximate 2-fold increase in conductance (Du et al., 2011). In previous studies, we showed that retigabine, the standard K_v7 channel opener, has depressant actions on spinal reflexes comparable to those obtained here for celecoxib (Rivera-Arconada et al., 2004; Vicente-Baz et al., 2016). Like celecoxib, retigabine has similar affinity for different K_v7 channel subunits and EC_{50} values in the low micromolar range (Tatulian et al., 2001; Wickenden et al., 2001).

The major proof obtained here in favour of the implication of K_v7 channels in mediating the spinal effects of celecoxib comes from the experiments with K_v7 channel blockers. Under the present conditions XE-991 showed clear potentiating actions on the firing of motor neurones, while effects on dorsal horn neurones were smaller. A minor effect of XE-991 on dorsal horn neurones has been previously observed in intracellular recordings obtained in rats (Rivera-Arconada and Lopez-Garcia, 2005). The lack of effect of XE-991 on cumulative depolarisation may be explained by the little impact that this compound has on dorsal horn neurones and, consequently, on their synaptic input to motor neurones.

The concentration of XE-991 used here was sufficient to produce complete blockade of the effects of the specific K_v7 openers ML213 and ICA-069673 in previous experiments (Vicente-Baz et al., 2016). We have also proof to our satisfaction that XE-991 does not prevent the effects of 1 μM diazepam, an allosteric modulator of GABA-A receptors under identical experimental conditions (not shown). Thus, we believe that the effects of XE-991 should be considered

effective and selective for K_v7 channels. Under these conditions of specific K_v7 channel blockade, celecoxib had no effect on spinal reflexes. Also relevant is the finding that XE-991 prevented the depressant effects of celecoxib on dorsal horn neurone's responses to C-fibre activation. This shows that early sensory processing of nociceptive information is depressed by celecoxib using a mechanism that likely involves K_v7 channels as well.

Further evidence supporting the implication of K_v7 channels on celecoxib depression of spinal nociceptive transmission was obtained in experiments with DMC, a structural analogue of celecoxib that lacks COX blocking activity (Kardosh et al., 2005). This compound produced depressant effects on spinal reflexes similar to those of celecoxib, that were also abolished by XE-991 application.

All these observations support a role for K_v7 channels on celecoxib action although a minor contribution of other targets might be possible. Celecoxib can interact with other targets like sodium and calcium channels which may also contribute to its observed effects (Brueggemann et al., 2009; Park et al., 2007). Although experiments with XE-991 may suggest direct actions on K_v7 channels, K_v7 channel blockade may depolarise resting potential originating an inactivation of sodium and calcium channels, also preventing celecoxib effects mediated by these other channels. We have shown previously that spinal neurones can be depolarised by the application of 10 μM XE-991 (Rivera-Arconada and Lopez-Garcia, 2005). Depolarisations ranged from 1 to 5 mV, with higher values found in motor neurones which also showed more negative potentials. These small depolarisations are unlikely to substantially affect high threshold calcium

channels or sodium channels to avoid subsequent actions of celecoxib. However, further studies will be necessary to definitively rule out this possibility.

In summary, the present results proof the concept that K_v7 channels are relevant potential mediators of the antinociceptive actions of celecoxib acting on the spinal cord. Although the results have to be interpreted cautiously due to the limitations of the present experimental approach, it is clear that celecoxib produces depression of sensory neurone's responses and spinal nociceptive reflexes activating non-specific targets. Although several non-specific targets have been identified, the present results are consistent with an involvement of K_v7 channels in these actions of celecoxib. In conclusion, we suggest that celecoxib may combine its main peripheral actions as COX's blocker with activity at K_v7 channels located in spinal nociceptive circuits to achieve analgesia.

Authorship Contributions:

Participated in research design: Lopez-Garcia, Rivera-Arconada

Conducted experiments: Vicente-Baz

Performed data analysis: Vicente-Baz, Rivera-Arconada

Wrote or contributed to the writing of the manuscript: Vicente-Baz, Lopez-Garcia, Rivera-Arconada

References

Blackburn-Munro G and Jensen BS (2003) The anticonvulsant retigabine attenuates nociceptive behaviours in rat models of persistent and neuropathic pain. Eur.J.Pharmacol. 460: 109-116.

Brueggemann LI, Mackie AR, Mani BK, Cribbs LL, Byron KL (2009) Differential effects of selective cyclooxygenase-2 inhibitors on vascular smooth muscle ion channels may account for differences in cardiovascular risk profiles. Mol.Pharmacol. 76: 1053-1061.

Clemett D and Goa KL (2000) Celecoxib: a review of its use in osteoarthritis, rheumatoid arthritis and acute pain. Drugs 59: 957-980.

Davies NM, McLachlan AJ, Day RO, Williams KM (2000) Clinical pharmacokinetics and pharmacodynamics of celecoxib: a selective cyclo-oxygenase-2 inhibitor. Clin.Pharmacokinet. 38: 225-242.

Dirig DM, Isakson PC, Yaksh TL (1998) Effect of COX-1 and COX-2 inhibition on induction and maintenance of carrageenan-evoked thermal hyperalgesia in rats. J.Pharmacol.Exp.Ther. 285: 1031-1038.

Du XN, Zhang X, Qi JL, An HL, Li JW, Wan YM, Fu Y, Gao HX, Gao ZB, Zhan Y, Zhang HL (2011) Characteristics and molecular basis of celecoxib modulation on K(v)7 potassium channels. Br.J.Pharmacol. 164: 1722-1737.

Frolov RV and Singh S (2014) Celecoxib and ion channels: a story of unexpected discoveries. Eur.J.Pharmacol. 730: 61-71.

Häring M, Zeisel A, Hochgerner H, Rinwa P, Jakobsson JET, Lönnerberg P, La Manno G, Sharma N, Borgius L, Kiehn O, Lagerström MC, Linnarsson S, Ernfors P (2018) Neuronal atlas of the dorsal horn defines its architecture and links sensory input to transcriptional cell types. Nat. Neurosci. 21: 869-880.

Hay C and de Belleroche J (1997) Carrageenan-induced hyperalgesia is associated with increased cyclo-oxygenase-2 expression in spinal cord. Neuroreport 8: 1249-1251.

Hedo G, Laird JM, Lopez-Garcia JA (1999) Time-course of spinal sensitization following carrageenan-induced inflammation in the young rat: a comparative electrophysiological and behavioural study in vitro and in vivo. Neuroscience 92: 309-318.

Herrero JF, Laird JM, Lopez-Garcia JA (2000) Wind-up of spinal cord neurones and pain sensation: much ado about something? Prog.Neurobiol. 61: 169-203.

Hirano K, Kuratani K, Fujiyoshi M, Tashiro N, Hayashi E, Kinoshita M (2007) Kv7.2-7.5 voltage-gated potassium channel (KCNQ2-5) opener, retigabine, reduces capsaicin-induced visceral pain in mice. Neurosci.Lett. 413: 159-162.

Inoue N, Ito S, Tajima K, Nogawa M, Takahashi Y, Sasagawa T, Nakamura A, Kyoi T (2009) Etodolac Attenuates Mechanical Allodynia in a Mouse Model of Neuropathic Pain. Journal of Pharmacological Sciences 109: 600-605.

Jentsch TJ (2000) Neuronal KCNQ potassium channels: physiology and role in disease. Nat.Rev.Neurosci. 1: 21-30.

Kalgutkar AS, Marnett AB, Crews BC, Remmel RP, Marnett LJ (2000) Ester and amide derivatives of the nonsteroidal antiinflammatory drug, indomethacin, as selective cyclooxygenase-2 inhibitors. J.Med.Chem. 43: 2860-2870.

Kardosh A, Wang W, Uddin J, Petasis NA, Hofman FM, Chen TC, Schönthal AH (2005) Dimethyl-celecoxib (DMC), a derivative of celecoxib that lacks cyclooxygenase-2-inhibitory function, potently mimics the anti-tumor effects of celecoxib on Burkitt's lymphoma in vitro and in vivo. Cancer Biol.Ther. 4: 571.

Kurumbail RG, Stevens AM, Gierse JK, McDonald JJ, Stegeman RA, Pak JY, Gildehaus D, Miyashiro JM, Penning TD, Seibert K, Isakson PC, Stallings WC (1996) Structural basis for selective inhibition of cyclooxygenase-2 by anti-inflammatory agents. Nature 384: 644-648.

Lee O and Seo Y (2008) The effects of intrathecal cyclooxygenase-1, cyclooxygenase-2, or nonselective inhibitors on pain behavior and spinal Fos-like immunoreactivity. Anesth.Analg. 106: 972-977.

Lizarraga I, Chambers JP, Johnson CB (2006) Depression of NMDA-receptor-mediated segmental transmission by ketamine and ketoprofen, but not L-NAME, on the in vitro neonatal rat spinal cord preparation. Brain Res. 1094: 57-64.

Lopez-Garcia JA and Laird JM (1998) Central antinociceptive effects of meloxicam on rat spinal cord in vitro. Neuroreport 9: 647-651.

Lucas S (2016) The Pharmacology of Indomethacin. Headache 56: 436-446.

Lucas-Romero J, Rivera-Arconada I, Roza C, Lopez-Garcia JA (2018) Origin and classification of spontaneous discharges in mouse superficial dorsal horn neurons. Sci.Rep. 8: 9735-11.

Malmberg AB and Yaksh TL (1992) Antinociceptive actions of spinal nonsteroidal anti-inflammatory agents on the formalin test in the rat. J.Pharmacol.Exp.Ther. 263: 136-146.

Mazo I, Roza C, Zamanillo D, Merlos M, Vela JM, Lopez-Garcia JA (2015) Effects of centrally acting analgesics on spinal segmental reflexes and wind-up. Eur.J.Pain 19: 1012-1020.

Mi Y, Zhang X, Zhang F, Qi J, Gao H, Huang D, Li L, Zhang H, Du X (2013) The role of potassium channel activation in celecoxib-induced analgesic action. PLoS One 8: e54797.

Nishiyama T (2006) Analgesic effects of intrathecally administered celecoxib, a cyclooxygenase-2 inhibitor, in the tail flick test and the formalin test in rats. Acta Anaesthesiol.Scand. 50: 228-233.

Park SY, Kim TH, Kim HI, Shin YK, Lee CS, Park M, Song JH (2007) Celecoxib inhibits Na+ currents in rat dorsal root ganglion neurons. Brain Res. 1148: 53-61.

Passmore GM, Selyanko AA, Mistry M, Al-Qatari M, Marsh SJ, Matthews EA, Dickenson AH, Brown TA, Burbidge SA, Main M, Brown DA (2003) KCNQ/M currents in sensory neurons: significance for pain therapy. J.Neurosci. 23: 7227-7236.

Penning TD, Talley JJ, Bertenshaw SR, Carter JS, Collins PW, Docter S, Graneto MJ, Lee LF, Malecha JW, Miyashiro JM, Rogers RS, Rogier DJ, Yu SS, AndersonGD, Burton EG, Cogburn JN, Gregory SA, Koboldt CM, Perkins WE, Seibert K, Veenhuizen AW, Zhang YY, Isakson PC (1997) Synthesis and biological evaluation of the 1,5-diarylpyrazole class of cyclooxygenase-2 inhibitors: identification of 4-[5-(4-methylphenyl)-3-(trifluoromethyl)-1H-pyrazol-1-yl]benze nesulfonamide (SC-58635, celecoxib). J.Med.Chem. 40: 1347-1365.

Rezende RM, Paiva-Lima P, Dos Reis WGP, Camêlo VM, Faraco A, Bakhle YS, Francischi JN (2012) Endogenous Opioid and Cannabinoid Mechanisms Are Involved in the Analgesic Effects of Celecoxib in the Central Nervous System. Pharmacology 89: 127-136.

Rivera-Arconada I and Lopez-Garcia JA (2005) Effects of M-current modulators on the excitability of immature rat spinal sensory and motor neurones. Eur.J.Neurosci. 22: 3091-3098.

Rivera-Arconada I, Martinez-Gomez J, Lopez-Garcia JA (2004) M-current modulators alter rat spinal nociceptive transmission: an electrophysiological study in vitro. Neuropharmacology 46: 598-606.

Rivera-Arconada I, Roza C, Lopez-Garcia JA (2016) Spinal Reflexes and Windup In Vitro: Effects of Analgesics and Anesthetics. CNS Neurosci.Ther. 22: 127-134.

Rivera-Arconada I, Roza C, Lopez-Garcia JA (2009) Enhancing m currents: a way out for neuropathic pain? Front.Mol.Neurosci. 2: 10.

Rome LH and Lands WE (1975) Structural requirements for time-dependent inhibition of prostaglandin biosynthesis by anti-inflammatory drugs. Proc. Natl. Acad. Sci. U.S.A. 72: 4863-4865.

Roza C, Mazo I, Rivera-Arconada I, Cisneros E, Alayón I, López-García J (2016) Analysis of spontaneous activity of superficial dorsal horn neurons in vitro: neuropathy-induced changes. Pflugers Arch - Eur J Physiol 468: 2017-2030.

Sathyamurthy A, Johnson KR, Matson KJE, Dobrott CI, Li L, Ryba AR, Bergman TB, Kelly MC, Kelley MW, Levine AJ (2018) Massively Parallel Single Nucleus Transcriptional Profiling Defines Spinal Cord Neurons and Their Activity during Behavior. Cell Rep. 22: 2216-2225.

Smith CJ, Zhang Y, Koboldt CM, Muhammad J, Zweifel BS, Shaffer A, Talley JJ, Masferrer JL, Seibert K, Isakson PC (1998) Pharmacological analysis of cyclooxygenase-1 in inflammation. Proc.Natl.Acad.Sci.U.S.A. 95: 13313-13318.

Sun Y, Dong Y, Wang Y, Zhao G, Lu G, Yang J, Wu S, Gu Z, Wang W (2013) Synergistic analgesia of duloxetine and celecoxib in the mouse formalin test: a combination analysis. PLoS ONE 8: e76603.

Tatulian L, Delmas P, Abogadie FC, Brown DA (2001) Activation of expressed KCNQ potassium currents and native neuronal M-type potassium currents by the anti-convulsant drug retigabine. J.Neurosci. 21: 5535-5545.

Vardeh D, Wang D, Costigan M, Lazarus M, Saper CB, Woolf CJ, Fitzgerald GA, Samad TA (2009) COX2 in CNS neural cells mediates mechanical inflammatory pain hypersensitivity in mice. J.Clin.Invest. 119: 287-294.

Vicente-Baz J, Lopez-Garcia JA, Rivera-Arconada I (2016) Effects of novel subtype selective M-current activators on spinal reflexes in vitro: Comparison with retigabine. Neuropharmacology 109: 131-138.

Wickenden AD, Zou A, Wagoner PK, Jegla T (2001) Characterization of KCNQ5/Q3 potassium channels expressed in mammalian cells. Br.J.Pharmacol. 132: 381-384.

Yamamoto T and Nozaki-Taguchi N (1996) Analysis of the effects of cyclooxygenase (COX)-1 and COX-2 in spinal nociceptive transmission using indomethacin, a non-selective COX inhibitor, and NS-398, a COX-2 selective inhibitor. Brain Res. 739: 104-110.

Zhang Y, Shaffer A, Portanova J, Seibert K, Isakson PC (1997) Inhibition of cyclooxygenase-2 rapidly reverses inflammatory hyperalgesia and prostaglandin E2 production. J.Pharmacol.Exp.Ther. 283: 1069-1075.

Zheng Q, Fang D, Liu M, Cai J, Wan Y, Han J, Xing G (2013) Suppression of KCNQ/M (Kv7) potassium channels in dorsal root ganglion neurons contributes to the development of bone cancer pain in a rat model. Pain 154: 434-448.

Zhu X and Eisenach JC (2003) Cyclooxygenase-1 in the spinal cord is altered after peripheral nerve injury. Anesthesiology 99: 1175-1179.

Footnotes

Financial support: This work was supported by the Spanish Ministry of Economy and Competitiveness (Grant No. SAF2016-77585-R) and the University of Alcala (Grant No. CCG2018/BIO-028). Jorge Vicente-Baz enjoys a fellowship from the University of Alcala.

Figure legends.

Figure 1. Actions of celecoxib on ventral root reflexes. Figure summarises celecoxib's effects on ventral root responses elicited by repetitive stimulation of the dorsal root at C-fibre intensity as obtained in spinal cords from inflamed mice. Original recordings in **A** show responses in control conditions (left) and after application of 10 μM celecoxib (right). In control conditions, repetitive stimulation (large vertical lines) originates a cumulative depolarisation in the DC channel associated to spike wind-up in the AC channel (gradual thickening of baseline). Note the depressant effects of celecoxib on both parameters. The original recordings in **B** show the MSR before and after application of celecoxib. Note the lack of effect of celecoxib on MSR amplitude. Arrows indicate the stimulus artefacts, that have been eliminated to improve visualization. In A and B three increasing concentrations were tested but only the maximal concentration used is shown. **C** and **D** show a quantification of spike counts (C) and amplitude (D) as obtained for each successive stimulus of the train (n = 10). Celecoxib produced a concentration-dependent reduction in spike wind-up and cumulative depolarisation. Graph in **E** summarises the effects of the three concentrations of celecoxib tested on the total spike counts ($F(3,27) = 16.02$; $p < 0.001$; One-way ANOVA) and the integrated area of the cumulative depolarisation ($F(3,27) = 18.45$; $p < 0.001$; One-way ANOVA). Asterisks indicate significant differences from pre-drug values using Bonferroni post-hoc test (** $p < 0.01$ and *** $p < 0.001$).

Figure 2. Celecoxib still depressed spinal reflexes after indomethacin application. Original recordings in **A** show the lack of effect of indomethacin ($p = 0.16$ for cumulative depolarisation and $p = 0.33$ for spike wind-up; paired *t*-test) and the subsequent actions of celecoxib. In the presence of indomethacin, celecoxib still produces a profound depression of nociceptive reflexes ($p = 0.01$ and $p = 0.04$ for cumulative depolarisation and spike wind-up, respectively; paired *t*-test). Graph in **B** summarises the results obtained in the six experiments made. # ($p < 0.05$) and ## ($p < 0.01$) stand for statistically significant differences between indomethacin and celecoxib values as obtained with paired *t*-test.

Figure 3. Implication of K_v7 channel modulation in the effects of celecoxib. Original recordings in **A** shows the lack of effect of celecoxib after K_v7 channel blockade with 10 µM XE-991. XE-991 applied during 90 min produced an increase in spike firing and then celecoxib (Cele), coapplied at three increasing concentrations, was devoid of effect. Graph in **B** summarizes results obtained in seven experiments. XE-991 increased firing ($p < 0.001$; paired *t*-test) with no effects on integrated area of the cumulative depolarisation ($p = 0.082$; paired *t*-test). In the presence of XE-991 no effects of celecoxib were observed ($F(3,18) = 2.0$; $p = 0.15$, for cumulative depolarisation and $F(3,18) = 0.3$; $p = 0.8$, for spike wind-up; One-Way ANOVA). Graph in **C** shows the results obtained in the four experiments in which celecoxib (10 µM) was applied after K_v7 channels blockade with linopirdine (Linop; 10 µM). Linopirdine on its own didn´t produce significant changes on spinal reflexes ($p = 0.069$ for cumulative depolarisation and $p = 0.075$ for spike wind-up; paired t-test). No depressant effects of

celecoxib either in cumulative depolarisation (p = 0.47; paired *t*-test) or spike wind-up (p = 0.81; paired *t*-test) were observed. $^{+++}$ indicate significant differences (p < 0.001) between pre-drug and XE-991 values.

Figure 4. Actions of the structural analogue DMC on nociceptive reflexes. Recordings in **A** illustrate the effects of 10 μM DMC on cumulative depolarisation (p = 0.014; paired *t*-test) and spike wind-up (p = 0.034; paired *t*-test), showing the same pattern of action than celecoxib. Pooled data from five experiments are shown in **B**. Graph in **C** summarises the results obtained in the three experiments that received DMC after K_V7 channels blockade with XE-991. XE-991 application increased spike wind-up (p = 0.014; paired *t*-test) and showed no effect on cumulative depolarisation (p = 0.15; paired *t*-test). Further application of DMC was devoid of effect. $^{+}$ indicates statistically significant differences (p < 0.05) from pre-drug values as obtained using paired *t*-test.

Figure 5. Effects of celecoxib on the activity of deep dorsal horn neurones. Image in **A** shows a drawing of a transverse section of the hemisected spinal cord (dorsal side up) with a reconstruction of its borders and laminar organization. The approximate location of the multielectrode shanks used for recording were recovered after DiI labelling. Dotted lines indicate the trajectory of the electrodes inside the spinal cord recovered from the seven experiments in which labelling with DiI was obtained. Original recordings in **B** show celecoxib (3 and 10 μM) effects on action potential firing in response to repetitive high intensity stimulation of the dorsal root as obtained from a deep dorsal horn

neurone. Figure **C** illustrate the lack of effect of celecoxib after K_v7 channel blockade with XE-991. Celecoxib at 3 and 10 µM was co-applied with 10 µM XE-991, but only the higher concentration is shown. Insets show the average of all action potentials in each condition. Calibration bars for all recordings: 0.2 mV and 2 s (0.2 mV and 1 ms for insets). Graph in **D** shows the effects of celecoxib on action potential firing in response to repetitive dorsal root stimulation in the 13 neurones tested. Celecoxib had depressant effects on neuronal firing ($F(2,24) = 15.28$; $p < 0.001$; One-way ANOVA). Vertical axis was broken to improve visualization. Graph **E** summarises the effects of celecoxib at 3 and 10 µM after K_v7 channel blockade with XE-991 in the five neurones tested. XE-991 increased the firing of deep dorsal horn neurones ($p = 0.026$; paired *t*-test). In the presence of XE-991, the coapplication of celecoxib was devoid of effect ($F(2,8) = 1.58$; $p = 0.26$; One-way ANOVA). For both graphs, values for individual neurones are shown in grey, mean ± SEM values for all neurones included in graph are indicated in black. Asterisks (** for $p < 0.01$ and *** for $p < 0.001$) and plus signs ($^+$ for $p < 0.05$) indicate statistically significant differences from pre-drug values as obtained using Bonferroni post-hoc test after One-way ANOVA or paired *t*-test, respectively.

Figure 6. Effects of celecoxib on the activity of superficial dorsal horn neurones. The microphotograph in **A** shows a transverse section of the spinal cord slice stained with toluidine (dorsal side up) with a reconstruction of its borders and laminar organization. The slice contained both sides of the spinal cord, but only one side is shown in the image for clarity. Original recordings in **B** show an example of the effects of 10 µM celecoxib on action potential firing. Figure **C**

illustrate the lack of effect of celecoxib after K_v7 channel blockade with XE-991. Insets show the average of all action potentials in each condition. Calibration bars for all recordings: 0.3 mV and 2 s (0.2 mV and 1 ms for insets). Graph in **D** shows the effects of celecoxib on action potential firing in response to repetitive dorsal root stimulation in the 12 neurones tested. Celecoxib had depressant effects on neuronal firing ($p < 0.001$; paired *t*-test). Graph in **E** summarises the effects of celecoxib at 10 µM after K_v7 channel blockade with XE-991 in the 9 neurones tested. XE-991 was devoid of effects, but prevented those of celecoxib. For both graphs, values for individual neurones are shown in grey, mean ± SEM values for all neurones included in graph are indicated in black. Asterisks (*** for $p < 0.001$) indicate statistically significant differences from pre-drug values as obtained using paired *t*-test.

Figure 1

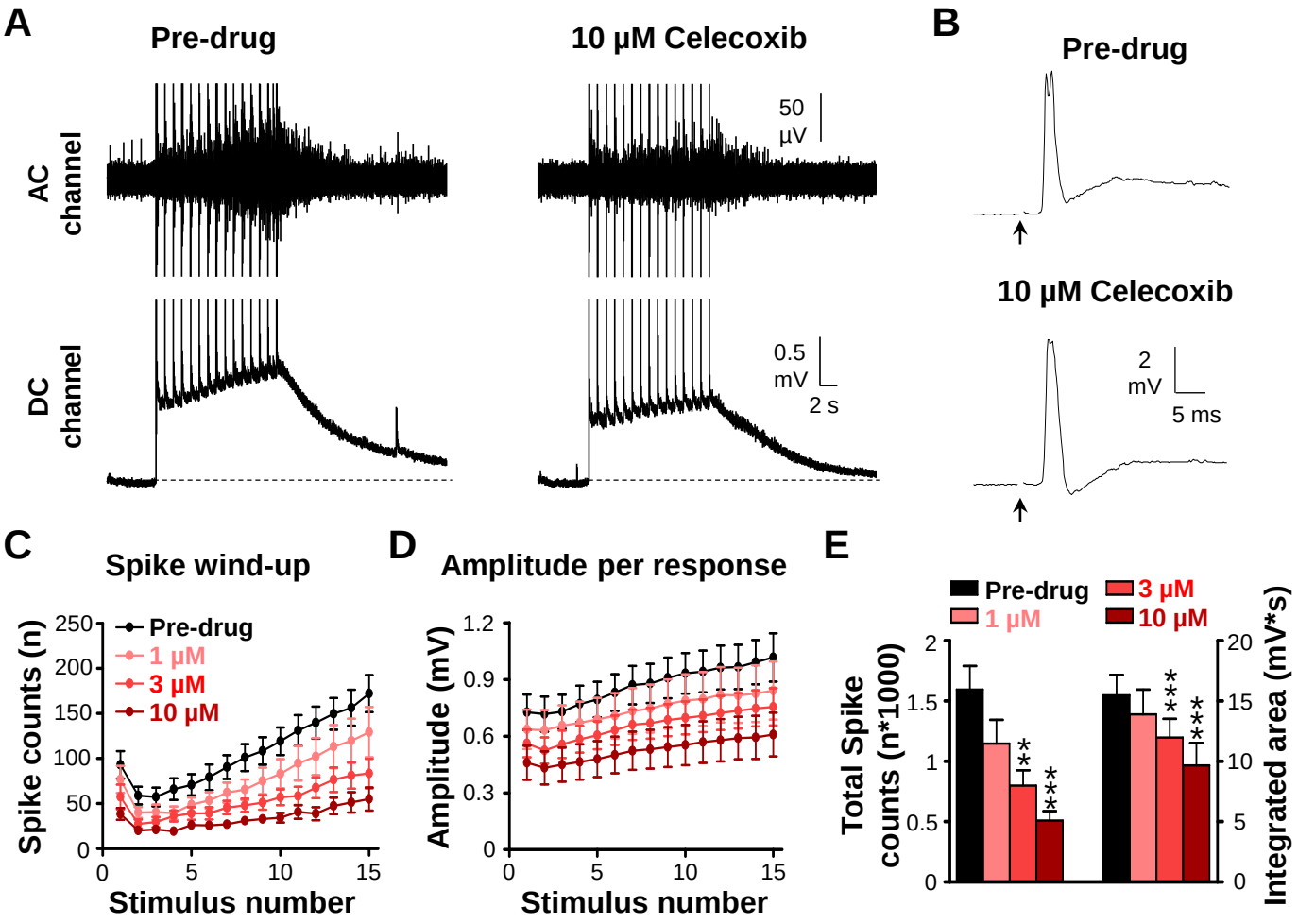
A
Pre-drug
10 μM Celecoxib
AC channel
DC channel
50 μV
0.5 mV
2 s
B
Pre-drug
10 μM Celecoxib
2 mV
5 ms
C
Spike wind-up
Spike counts (n)
Pre-drug
1 μM
3 μM
10 μM
Stimulus number
D
Amplitude per response
Amplitude (mV)
Stimulus number
E
Pre-drug
1 μM
3 μM
10 μM
Total Spike counts (n*1000)
Integrated area (mV*s)

Figure 2

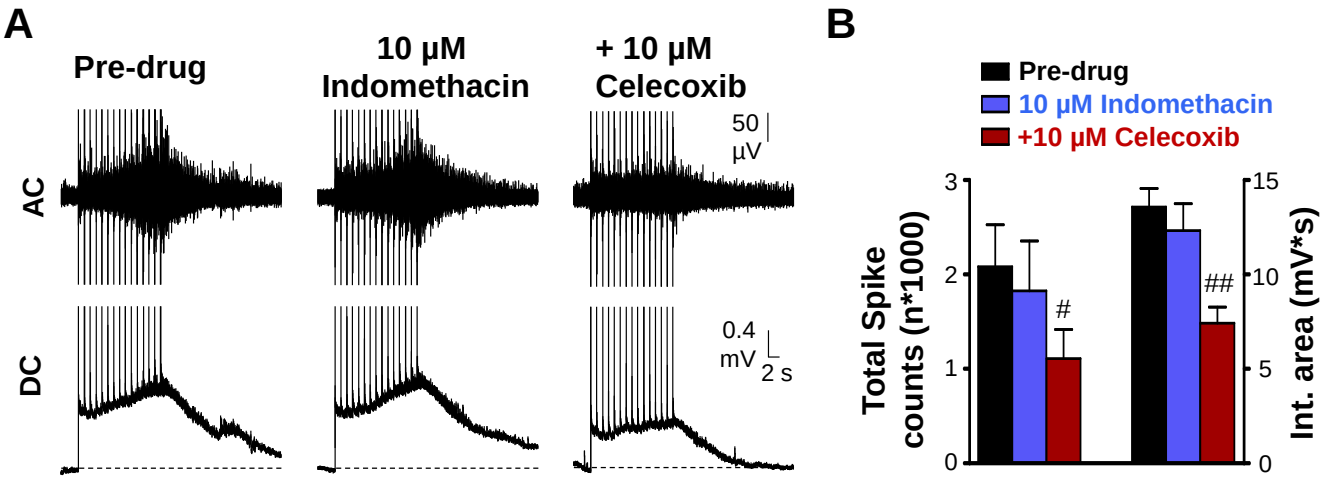
A
Pre-drug
10 μM Indomethacin
+ 10 μM Celecoxib
AC
DC
50 μV
0.4 mV
2 s
B
Pre-drug
10 μM Indomethacin
+10 μM Celecoxib
Total Spike counts (n*1000)
Int. area (mV*s)
#
##
0
1
2
3
0
5
10
15

Figure 3

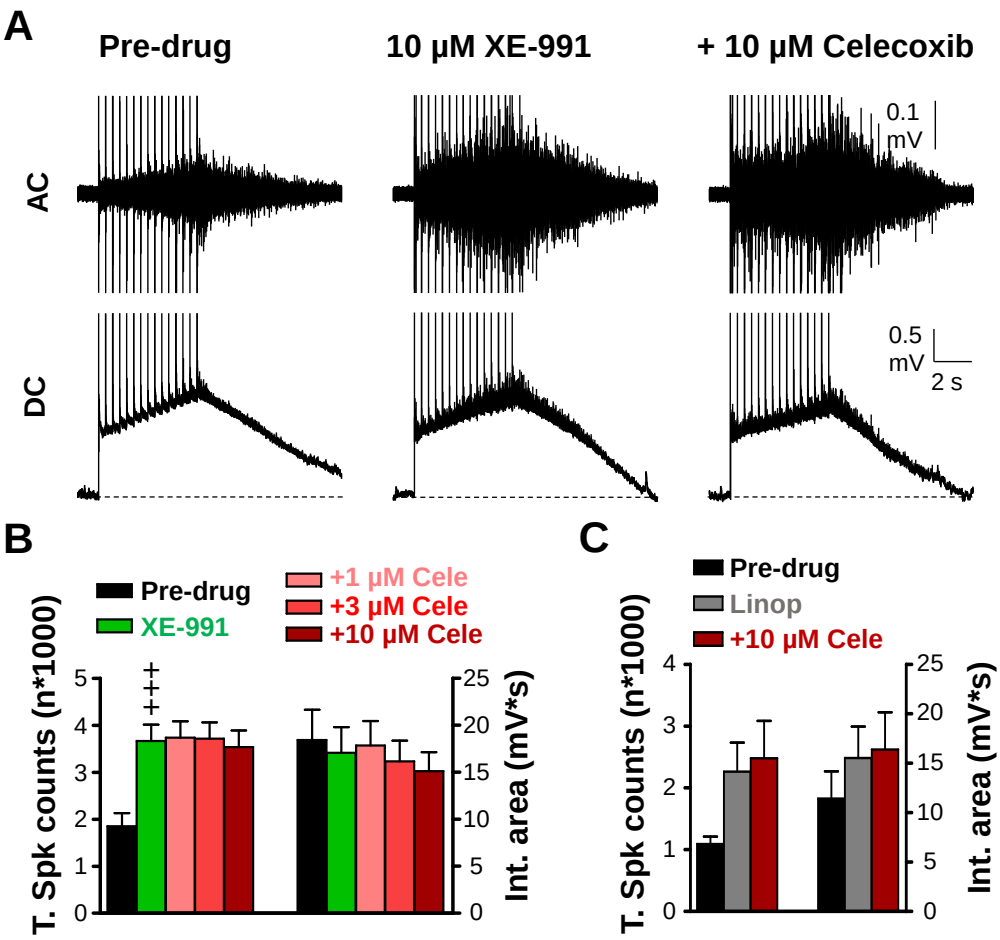
A
Pre-drug
10 μM XE-991
+ 10 μM Celecoxib
AC
DC
0.1 mV
0.5 mV
2 s
B
Pre-drug
XE-991
+1 μM Cele
+3 μM Cele
+10 μM Cele
T. Spk counts (n*1000)
Int. area (mV*s)
C
Pre-drug
Linop
+10 μM Cele
T. Spk counts (n*1000)
Int. area (mV*s)

Figure 4

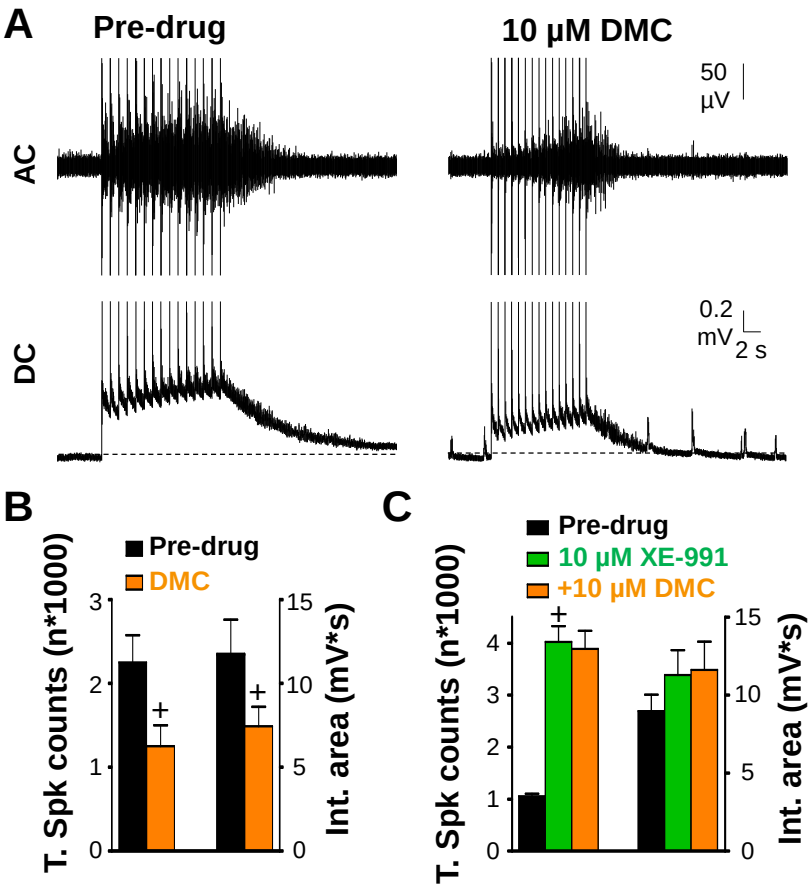
A
Pre-drug
10 µM DMC
AC
DC
50 µV
0.2 mV
2 s
B
Pre-drug
DMC
T. Spk counts (n*1000)
Int. area (mV*s)
C
Pre-drug
10 µM XE-991
+10 µM DMC
T. Spk counts (n*1000)
Int. area (mV*s)

Figure 5

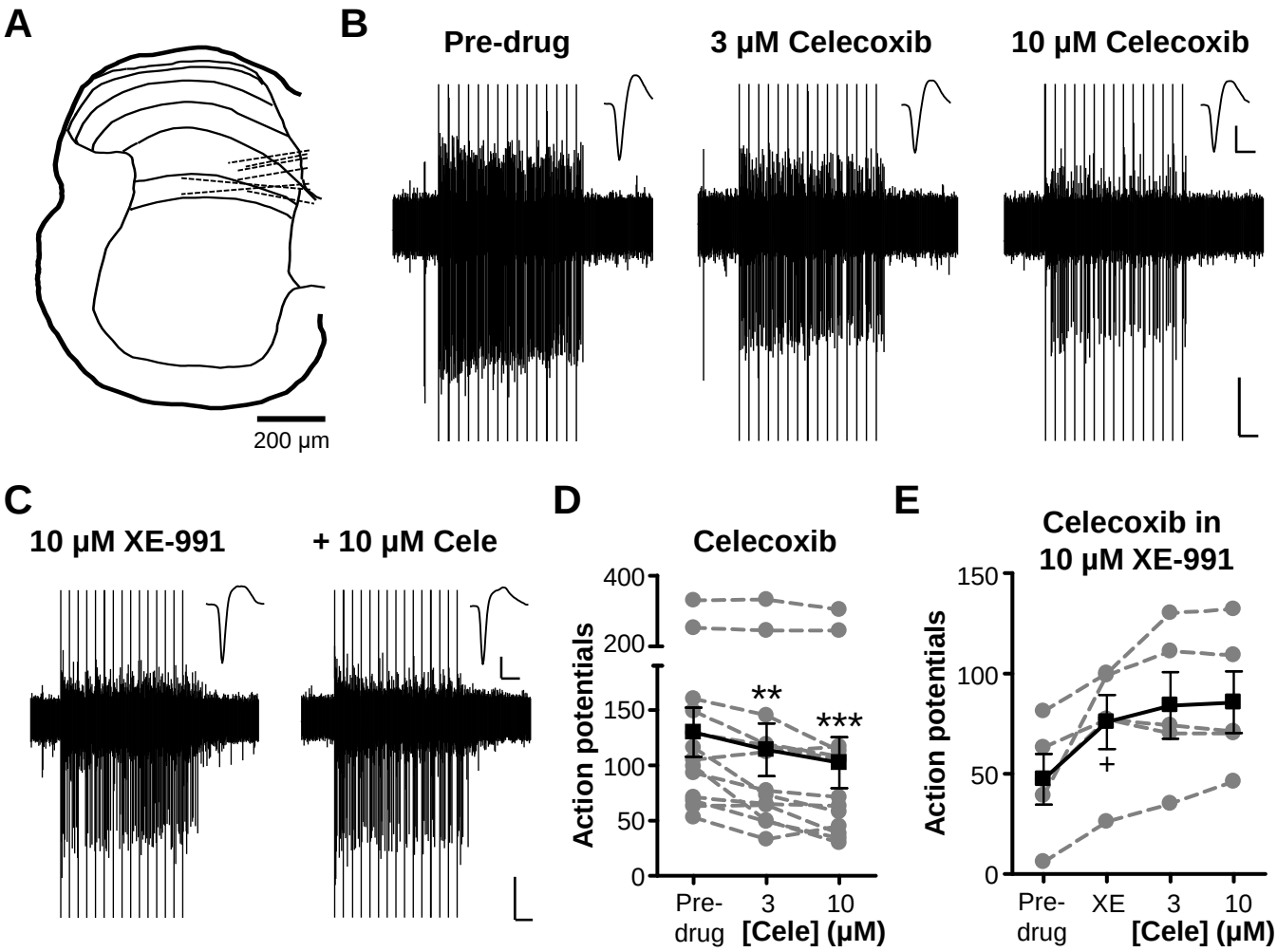
A
200 µm
B
Pre-drug
3 µM Celecoxib
10 µM Celecoxib
C
10 µM XE-991
+ 10 µM Cele
D
Celecoxib
Action potentials
400
200
150
100
50
0
**
***
Pre-drug
3
10
[Cele] (µM)
E
Celecoxib in
10 µM XE-991
Action potentials
150
100
50
0
+
Pre-drug
XE
3
10
[Cele] (µM)

Figure 6

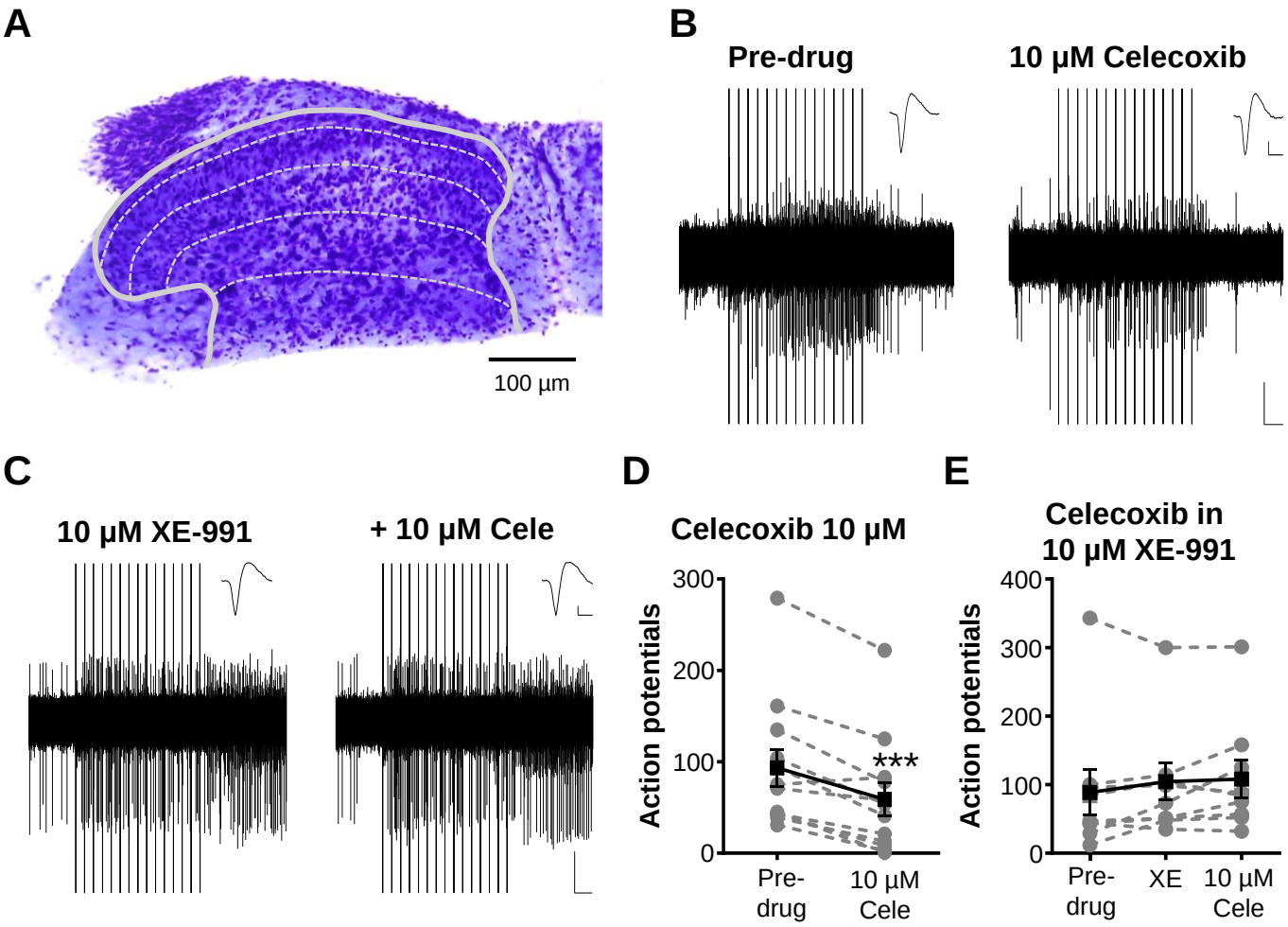
A
100 µm
B
Pre-drug
10 µM Celecoxib
C
10 µM XE-991
+ 10 µM Cele
D
Celecoxib 10 µM
Action potentials
300
200
100
0
***
Pre-drug
10 µM Cele
E
Celecoxib in 10 µM XE-991
Action potentials
400
300
200
100
0
Pre-drug
XE
10 µM Cele